Mon. Not. R. Astron. Soc. **373,** 79–94 (2006) doi:10.1111/j.1365-2966.2006.10950.x

The Macquarie/AAO/Strasbourg Hα Planetary Nebula Catalogue: MASH

Quentin A. Parker,[1,2⋆] A. Acker,[3] D. J. Frew,[1] M. Hartley,[4] A. E. J. Peyaud,[1,3] F. Ochsenbein,[3] S. Phillipps,[5] D. Russeil,[6] S. F. Beaulieu,[7] M. Cohen,[8] J. Köppen,[3] B. Miszalski,[1] D. H. Morgan,[9] R. A. H. Morris,[5] M. J. Pierce[1,5] and A. E. Vaughan[1]

[1]*Department of Physics, Macquarie University, Sydney, NSW 2109, Australia*
[2]*Anglo-Australian Observatory, Epping, NSW 1710, Australia*
[3]*Observatoire Astronomique, Université Louis Pasteur, 67000 Strasbourg, France*
[4]*UK Schmidt Telescope, Anglo-Australian Observatory, Siding Spring, 2357 NSW, Australia*
[5]*Astrophysics Group, University of Bristol, Tyndall Avenue, Bristol BS8 1TL*
[6]*Laboratoire d'Astrophysique de Marseille, 2 Place Le Verrier, 13248 Marseille Cedex 04, France*
[7]*Département de Physique, et Observatoire du mont Mégantic, Université Laval, Québec, QC, Canada G1K 7P4*
[8]*Radio Astronomy Laboratory, University of California, Berkeley, CA 94720, USA*
[9]*Institute for Astronomy, School of Physics, University of Edinburgh, Edinburgh EH8 3HJ*

Accepted 2006 August 15. Received 2006 August 4

ABSTRACT

We present the Macquarie/AAO/Strasbourg Hα Planetary Nebula Catalogue (MASH) of over 900 true, likely and possible new Galactic planetary nebulae (PNe) discovered from the AAO/UKST Hα survey of the southern Galactic plane. The combination of depth, resolution, uniformity and areal coverage of the Hα survey has opened up a hitherto unexplored region of parameter space permitting the detection of this significant new PN sample. Away from the Galactic bulge the new PNe are typically more evolved, of larger angular extent, of lower surface brightness and more obscured (i.e. extinguished) than those in most previous surveys. We have also doubled the number of PNe in the Galactic bulge itself and although most are compact, we have also found more evolved examples. The MASH catalogue represents the culmination of a seven-year programme of identification and confirmatory spectroscopy. A key strength is that the entire sample has been derived from the same, uniform observational data. The 60 per cent increase in known Galactic PNe represents the largest ever incremental sample of such discoveries and will have a significant impact on many aspects of PN research. This is especially important for studies at the faint end of the PN luminosity function which was previously poorly represented.

Key words: astronomical data bases: miscellaneous – catalogues – surveys – planetary nebulae: general.

1 INTRODUCTION

Planetary nebulae (PNe) are a common end-point of stellar evolution. They are among the most complex, varied and fascinating of celestial phenomena and a large fraction of all stars between 1 and 8 $M_{\odot}$ will become observable PNe towards the end of their lifetimes. PNe are a brief, still poorly understood evolutionary phase, lasting for a mere 30 000–70 000 yr (e.g. Zijlstra & Pottasch 1991). This brevity has limited the number of objects for study and restricted the scope for unravelling their full characteristics and evolutionary diversity. However, PNe hold the key to determining the physics and time-scales of mass-loss and evolution for low- to intermediate-mass stars (Iben 1995). They are also vital probes of nucleosynthesis processes, abundance gradients and the chemical enrichment of the interstellar medium (ISM), and act as powerful tracers of our Galaxy's star-forming history (e.g. Maciel & Costa 2003). However, due to the relatively small numbers previously known (i.e. ∼1500) compared to those expected to populate the Galaxy's disc (e.g. ∼23 000, Zijlstra & Pottasch 1991; or ∼30 000–35 000 for the whole galaxy, Frew & Parker 2005; Peyaud 2005) their potential as tracers of Galactic structure and as windows to stellar evolution in the critical phase from PN to white dwarf, has only been partially realized.

Unfortunately, previous PN catalogues represent an extremely heterogeneous collection from over 75 yr of diverse searches

⋆E-mail: qap@ics.mq.edu.au

undertaken with a host of different telescopes and detection techniques. They are listed in the catalogues by Perek & Kohoutek (1967) and Kohoutek (2001), but without a full examination of the status of the 1500 objects they classified as PNe. The Strasbourg/ESO catalogue of Galactic PNe (Acker et al. 1992; Acker, Marcout & Ochsenbein 1996) is based on a detailed spectrophotometric survey of existing data plus observations of about 1100 PNe (from ESO and OHP telescopes from 1984 to 1991 by Stenholm and Acker). This allowed the spectral analysis of 1385 true PNe (about 15 papers between 1990 and 1992), the classification of 489 possible PNe, and the study of 330 misclassified PNe.

However, these samples remain particularly deficient in examples of both highly evolved and faint but compact objects. Hence the picture of stellar evolution from the asymptotic giant branch (AGB) to post-AGB star, proto-PN, mature and senile PN remains incomplete. A significant number of known Galactic PNe have come from dedicated searches using modest aperture telescopes often equipped with objective-prisms (e.g. Henize 1967). Another key source has been from searches of large wide-field Schmidt telescope direct or objective-prism exposures (e.g. Melmer & Weinberger 1990; Kerber, Lercher & Weinberger 1996; Kerber et al. 1998).

Generally, progress in advancing Galactic PN numbers has been slow and piecemeal with papers dedicated to a few discoveries common, such as Weinberger, Kerber & Groebner (1997) with three PNe and Beer & Vaughan (1999) with two PNe. Some of these discoveries are serendipitous, for example, Kraan-Korteweg et al. (1996), who found two new PNe while searching for obscured galaxies in the southern Galactic plane. Several newer, targeted PN programmes are based on CCD narrow-band imaging in regions like the Galactic bulge, where expected number densities are high. These have revealed significant new PNe over the relatively small areas that can be surveyed though the numbers remain modest, for example, Beaulieu, Dopita & Freeman (1999) with 56 new PNe, and Boumis et al. (2003) with 25 PNe.[1] Other programmes have made use of the specific IRAS colours of PN candidates through the far-infrared excess associated with the warm dust in the nebulae (e.g. Ratag & Pottash 1991; Van de Steene & Pottash 1995 who identified 63 new PNe and 67 possible PNe). There is always a question mark over such candidates until confirmatory spectroscopy and higher resolution optical/near-infrared or radio imaging are obtained. Jacoby & van de Steene (2004) used near-infrared [S III]λ9532 Å imaging over a 4 $\times$ 4-deg^2 region of the Galactic bulge to uncover 94-candidate PNe of which 63 were spectroscopically confirmed.

We now report an important new source of Galactic PNe found *solely* from the Anglo-Australian Observatory UK Schmidt Telescope (AAO/UKST) Hα survey (Parker et al. 2005). This is the Macquarie/AAO/Strasbourg Hα Catalogue of Galactic PNe (MASH). These discoveries originate from the same observational data, yielding the largest ever incremental increase in Galactic PN numbers and presenting the least biased, and most homogeneous sample of PNe yet created over the widest evolutionary range. In this paper we present the basic catalogue of 905 new Galactic PNe comprising 578 true PNe (64 per cent), 186 likely PNe (21 per cent) and 141 possible PNe (15 per cent). We briefly describe the discovery technique, spectroscopic follow-up and confirmation, morphological classification, basic statistics and a few current MASH highlights. Detailed investigations of the sample will be presented in an upcoming series of papers.

[1] Many of the Boumis et al. PNe were also independently discovered by our programme between 1998 and 2001 and reported on the CD-ROM in 2001 (Parker et al. 2001, 2003).

2 THE DISCOVERY MEDIUM: THE AAO/UKST Hα SURVEY

In 2003 the AAO/UKST completed a high spatial resolution ($\sim$1 arcsec), narrow-band [70 Å FWHM (full width at half-maximum)], Hα + [N II]$\lambda\lambda$6548, 6583 Å survey of the southern Galactic plane using the world's largest optical interference filter for astronomy with a clear aperture of 305 mm (Parker & Bland-Hawthorn 1998) with fine-grained Tech-Pan film as detector (Parker & Malin 1999). Approximately 4000 deg^2 of the Southern Milky Way was covered to $|b| \sim 10^\circ$–13° with 233 survey fields on 4° centres (e.g. see fig. 1 of Parker et al. 2005). This survey of Galactic emission has a combination of coverage, resolution, uniformity and sensitivity superior to previous surveys of this type (Parker & Phillipps 1998; Parker et al. 2005). The SuperCOSMOS microdensitometer (Hambly et al. 2001a) scanned the Hα survey exposures and their matching, contemporaneous, broad-band SR (short red RG630 filter) exposures at 10 μm (0.67 arcsec) resolution. The survey is now available online in digital form as the SuperCOSMOS Hα Survey (SHS).[2] The survey has a faint sensitivity limit of 5 Rayleighs at Hα (Parker et al. 2005) equivalent to $\sim$2.4 $\times$ 10^{-17} erg cm^{-2} s^{-1} arcsec^{-2}, and, as a consequence, has revealed an enormous variety of discrete, hitherto unknown emission nebulosities, including an unprecedented sample of faint, new PNe over the entire southern Galactic plane (Parker & Phillipps 1998; Parker et al. 2003). A significant fraction of these are compact PNe in the heavily crowded Galactic bulge region (Peyaud 2005).

The sensitivity and arcsecond resolution of the SHS makes it a particularly powerful discovery tool, invaluable for investigating the detailed structures of emission features across the widest range of angular scales. More specifically it is capable of revealing fine morphological detail of our new PNe. MASH PNe are also less affected by dust and so are easier to detect than via traditional [O III] imaging in more obscured regions of the Galactic plane. Importantly, our discoveries are not simply more of what is known in previous catalogues. A significant fraction represent the most senile stages of PN evolution, dominating the population at the faint end of the PN luminosity function (PNLF). MASH remedies a deficiency of observational data on evolved PNe (Tweedy & Kwitter 1996; Xilouris et al. 1996) and those interacting with the ISM (see Pierce et al. 2004 and Frew & Parker, in preparation). Note that known PNe are also very well imaged in the new survey permitting the discovery of additional, faint outer structures.

3 MASH DISCOVERY TECHNIQUES

The bulk of MASH PNe have been discovered from careful visual scrutiny of the original Hα survey material under a microscope on a field-by-field basis by at least two members of the scanning team led by QAP, MH and DR (leading to the PHR prefix for most MASH PNe). The process began in 1998 and all 233 survey fields, each of which effectively covered $\sim$25 deg^2, were scanned by early 2003. In Fig. 1 we present 4 $\times$ 4 arcmin^2 Hα, SR and quotient (i.e. Hα divided by SR) images of a typical example of a new PN discovered in this way. Visual scanning was effective at finding resolved ($\geqslant$6 arcsec) candidate PNe on the basis of morphology, isolation

[2] http://www-wfau.roe.ac.uk/sss/halpha/

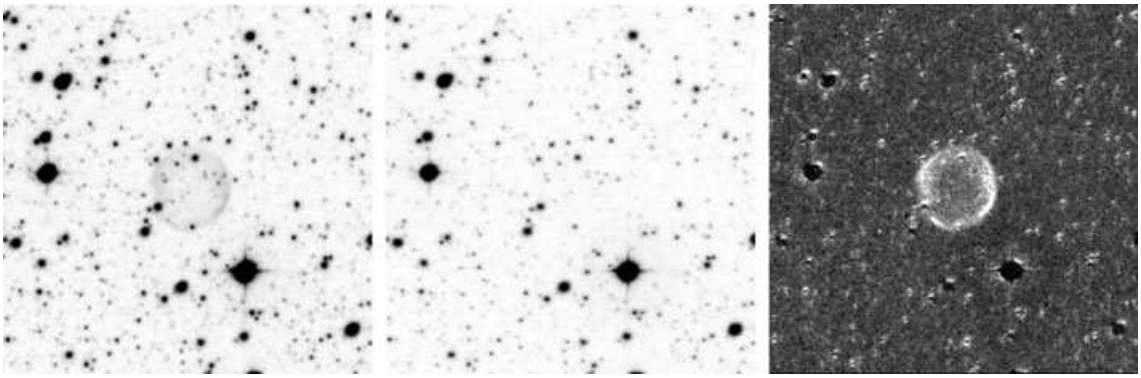

Figure 1. 4 × 4 arcmin^2 extracts of SuperCOSMOS data around a newly discovered PN (PHR1520−5243) from the 3-h Hα survey data (a – left-hand panel), matching 15-min Tech-Pan short red SR data (b – middle panel) and simple quotient image (c – right-hand panel). The new PN is 53 arcsec in diameter and is only visible in the Hα image. Note the well matched depth for point sources between the two exposures and lack of an obvious central star candidate.

and identification as an Hα nebulosity. These objects neither resemble stars (unless they are unresolved/barely resolved) nor, usually, galaxies because of their more varied and occasionally fractured morphologies, lack of a central extended bulge and their location in dense star fields. Because of this and their low surface brightness, PNe would not normally be detectable as discrete sources via standard star/galaxy separation techniques that can be applied to the parametrized SuperCOSMOS pixel data produced from the Hα survey film scans (e.g. Hambly et al. 2001a).

Once the SHS pixel data became fully available in 2003 it was possible to check all the previous visual identifications and in particular to obtain more accurate estimates of nebular size, position and morphology (see Section 5.1). MASH catalogue entries have been completely updated in this way and the current MASH release represents a far more consistent and accurate description for the new PNe compared to what was available in the preliminary CD-ROM issued in 2001.[3] This catalogue has been completely superceded with many contaminating sources such as H II regions removed and significant numbers of PNe added.

As the FWHM of the Hα filter bandpass is 70 Å with a central wavelength of 6590 Å, it is more accurately an Hα + [N II]$\lambda\lambda$6548, 6583 filter. This is an advantage for PN searches based around the Hα line as many Type I PNe can have [N II] $\gg$ Hα by up to a factor of 10 or more (e.g. Corradi et al. 1997). Note the central filter wavelength is redward of Hα to account for the scanning down of wavelength with off-axis flux as the filter encounters the f/2.48 converging beam of the UKST. The seasonal and nightly extreme temperature variations of -5 to 30°C at the UKST throughout the survey period only result in a maximum 1.23 Å shift of the central wavelength which is small in comparison to the filter bandpass (Parker & Bland-Hawthorn 1998).

3.1 Difference imaging

Another significant advantage of the SuperCOSMOS Hα and SR online pixel data were the ability to perform simple quotient (Hα and SR image division) or more sophisticated difference imaging directly on the digital data. This is an effective means of revealing the underlying nebulosity (e.g. see Fig. 1). When difference imaging is applied to large areas of digital data from a single survey field it becomes an effective discovery technique in its own right, particularly in highly crowded star fields where very faint diffuse emission or small, compact nebula are otherwise hard to detect.

Many additional bulge PNe were discovered in this way by use of a sophisticated, innovative difference imaging technique developed by Bond et al. (2001). It is based on variable point spread function (PSF) matching between the Hα and equivalent broad-band red SuperCOSMOS pixel data. This technique is available from the Wide Field Astronomy Unit (WFAU) with prior arrangement as its use is quite computationally intensive, especially when applied to the large image areas where it works best. This is a powerful alternative to image moment and deblending algorithms which are often misled by severe field crowding and yields better performance than simple quotient imaging. In Fig. 2 we present three typical examples of new compact bulge PNe uncovered in this fashion. This technique has been used on 18 dense bulge fields to reveal 137 new PNe (e.g. Peyaud, Acker & Parker 2003, 2004; Peyaud 2005).

These new PNe have been subsequently confirmed spectroscopically (Section 4) and were unknown to Acker et al. (1992, 1996). They complement the other significant sample of ∼350 new MASH bulge PNe found solely from the visual scans of the original survey films by QAP which were generally more extended. Compact emitters found in the bulge from the difference imaging are not all new PNe. Contaminants such as symbiotic stars or other emission-line stars are usually identified by their subsequent spectral signatures (refer to Section 4.1). These have their own scientific value and will be analysed separately.

3.2 Blocked-down survey images

A final technique was applied to the Hα survey data in the hunt for extremely low surface brightness and large angular scale PNe. DJF and QAP performed a careful systematic visual search of 16 × 16 (11 arcsec resolution) blocked-down FITS data of all 233 survey fields. These blocked-down fields are available individually online for download from the SHS web site (see footnote 2) and have an accurate WCS coordinate system built into their FITS headers. The blocking has the beneficial effect of making large, coherent, extremely low surface brightness nebulosity easier to detect. This has revealed many additional large-scale faint candidate PNe and other nebulosities [including many supernova remnant (SNR) candidates], which have formed the basis for further spectroscopic

[3] Formerly known as the Edinburgh/AAO/Strasbourg Hα PN catalogue.

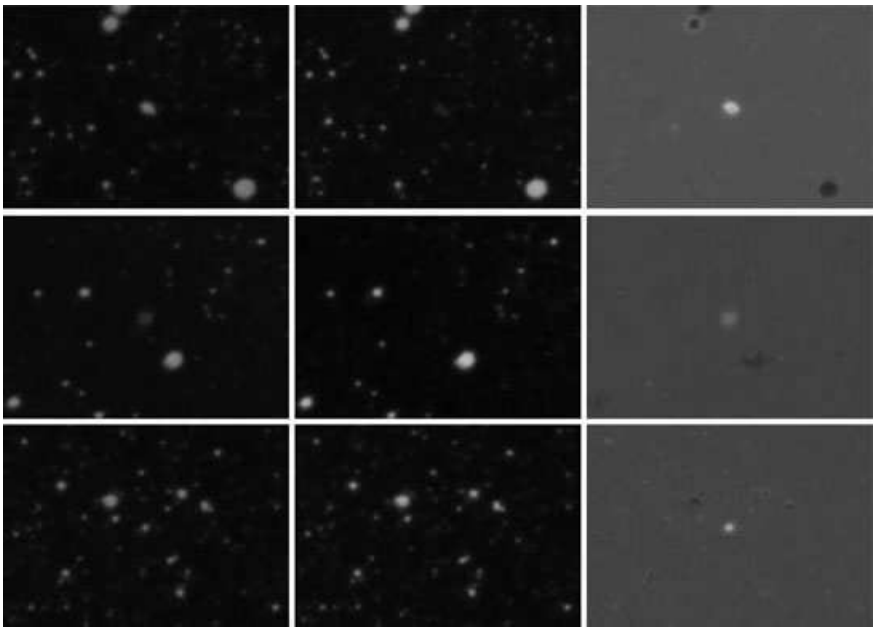

Figure 2. 1×1.4 arcmin^2 extracts of SuperCOSMOS data around three newly discovered PNe in the Galactic bulge from the 3-h Hα survey data (a – left-hand column), matching 15 min Tech-Pan SR data (b – middle column) and difference image based on application of the PSF matching scheme of Bond et al. (2001) (c – right-hand column). This has proven to be particularly effective in uncovering a significant number of compact, new, bulge PNe (e.g. Peyaud 2005).

follow-up. Such additional confirmed and possible PNe are identified by the FP prefix in the catalogue.

3.3 Completeness

We consider that practically all large ($\geqslant 4$ arcmin) PNe visible in the survey data have now been catalogued. However, we have undoubtedly missed extremely faint, low surface brightness and/or compact PNe during our visual scans of the original SHS films. The SHS online data now affords additional opportunities to uncover very low surface brightness small-scale PN candidates via difference imaging (as we have already performed on the bulge fields). Furthermore, a significant number of faint, compact, star-like PNe await to be uncovered. The SuperCOSMOS image analysis mode (IAM) parametrized data (e.g. Hambly et al. 2001a) can be used to trawl for such compact PNe (along with emission-line stars) from the IAM photometry and specifically H$\alpha - R$ versus $R - I$ colour–colour plots. Note that to do this the independent UKST I-band survey data, available as a separate online SuperCOSMOS survey, is incorporated by matching the IAM positional information to that of the Hα and R-band IAM data. Several PNe have already been found in this way (e.g. Pierce 2005; Hopewell et al., in preparation) and three are included in MASH. We estimate there may be 200–400 compact PNe with $R < 20.5$ awaiting discovery based on the numbers found in half a dozen SHS fields analysed in this way. We are also undertaking a new search of the SHS digital data in quotient form which is uncovering many new compact PN candidates and occasional extremely low surface brightness candidates also. These new MASH PNe, once confirmed, will comprise the first MASH supplement. Note that the SHS also overlaps at the equator with the IPHAS Northern Hα survey counterpart currently underway on the INT 2.5-m telescope on La Palma (Drew et al. 2005) which promises to deliver an equivalent increase in PNe in the northern Galactic plane (Corradi et al. 2005).

4 SPECTROSCOPIC CONFIRMATION OF MASH PN CANDIDATES

An extensive programme of optical follow-up spectroscopy was undertaken between 1998 and 2005 on a series of 2-m class telescopes, object by object, for the entire sample of candidate PNe amounting to 32 individual observing missions. The resultant spectra were evaluated against specific emission-line and other criteria before the PN was accepted as genuine by QAP/AA and later QAP/DJF. The work was largely carried out at the Strasbourg Observatory and Macquarie University between 2001 and 2005.

Even if the imagery alone was convincing, spectroscopy is still required to provide valuable additional information such as velocity (kinematic and, where possible, nebular expansion), excitation class, line fluxes and ratios for nebula temperature and density estimates. Most of the detailed spectroscopic information derived from these observations will be reported in subsequent publications in this series.

The spectroscopic data have a variety of resolutions and wavelength coverage depending on the telescope and instrumentation available as summarized in Table 1. Often, there are several different spectra available for a given PN from different runs on the same telescope, or from different telescopes at different resolutions and across different parts of the nebula. Some of these exhibit fluctuations in relative line strengths, perhaps because different ionization zones have been sampled across these extended PNe by spectrograph slit or fibre. Such repeat observations permit estimations of consistency of flux calibration, line ratios and radial velocities. When the same telescope and grating was used in different seasons the observed instrumental resolution can still shift slightly due to minor hardware adjustments and difficulties in obtaining and maintaining optimum spectrograph focus, especially during rapid temperature variations through the night.

In the particularly rich bulge fields, effective use was made of the UKST FLAIR-II (e.g. Morgan & Parker 1998) and then the 6dF (Watson, Parker & Miziarski 1998) multi-object spectroscopy

Table 1. Summary details of the extensive MASH spectroscopic follow-up programme.

Telescope	Run dates (dd–dd mm yyyy)	Instrument	Wavelength (range Å)	Resolution (Å FWHM)	Grating	Exposure times (s)	Observer
MSSSO 2.3 m	02 07 1998	DBS B/R	3820–5680; 5290–6850	4.6/2.3	300B/600R	600–900	QAP/MH
UKST 1.2 m	22 07 1998	FLAIR B/R	4300–5800; 5900–7100	4.7/4.6	600V/600R	3 × 1800	QAP
UKST 1.2 m	11 08 1998	FLAIR B/R	4350–5780; 5810–7220	5.4/4.2	600V/600R	3 × 1800	QAP
SAAO 1.9 m	12–18 01 1999	CCD SPEC	3790–7700	5.9	300B	600–900	QAP/DR
UKST 1.2 m	07–11 07 1999	FLAIR B/R	3900–7200; 6310–7030	11.0/2.4	250B/1200R	3 × 1800	QAP
UKST 1.2 m	12–13 08 1999	FLAIR R	6310–7030	2.4	1200R	3 × 1800	QAP
MSSSO 1.9 m	04–09 01 2000	B& C CCD	5650–6785	2.0	600R	600–1200	QAP/MH
UKST 1.2 m	04–09 01 2000	FLAIR	3920–7350; 6270–7050	12.0/2.7	250B/1200R	3 × 1800	QAP
UKST 1.2 m	04–05 07 2000	FLAIR	6200–6940	2.8	1200R	3 × 1800	QAP
SAAO 1.9 m	08–15 02 2000	CCD SPEC	3790–7780	7.0	300B	600–900	QAP
SAAO 1.9 m	20–27 06 2000	CCD SPEC	3800–7800	7.2	300B	600–900	QAP/RAHM
MSSSO 2.3 m	01–06 07 2000	DBS B/R	4000–5940; 6060–7020	2.4/1.3	600B/1200R	600–1200	QAP/MH
ESO 1.5 m	03 07 2000	B & C CCD	2680–8050	5.6	300B	600–900	DR/SB
SAAO 1.9 m	15–21 05 2001	CCD SPEC	3810–7800	7.1	300B	600–900	QAP/SB
MSSSO 2.3 m	22–27 06 2001	DBS B/R	4320–6220; 5930–6870	2.5/1.3	600B/1200R	600–1200	RAHM/MH
MSSSO 2.3 m	06–10 07 2002	DBS B/R	4320–6240; 6180–7100	2.3/1.3	600B/1200R	600–1200	MH/AEV/SB
SAAO 1.9 m	16–22 07 2002	CCD SPEC	3240–7270	7.1	300B	600–900	QAP/RAHM
OHP 1.9 m	08–11 11 2002	CARELEC	3800–7500	7	150B	3 × 1200	DR/AA
SAAO 1.9 m	28 01 2003 to 01 02 2003	CCD SPEC	3230–7260	7.1	300B	600–900	QAP/RAHM
MSSSO 2.3 m	04–07 07 2003	DBS B/R	3870–5600; 6170–7110	2.5/1.2	600B/1200R	600–1200	RAHM/SB
SAAO 1.9 m	24–30 06 2003	CCD SPEC	3360–7520; 6150–6880	5.0/1.3	300B/1200R	600–900	QAP/AEJP
UKST 1.2 m	16–21 08 2003	6DF V/R	3920–5530; 5330–7590	4.9/5.8	580V/425R	3 × 1800	QAP/AEJP
OHP 1.9 m	23–26 09 2003	CARELEC	3800–7500	7	150B	3 × 1200	AA/DR
MSSSO 2.3 m	24–27 01 2004	DBS B/R	3870–5600; 6170–7110	2.5/1.2	600B/1200R	600–1200	DJF
SAAO 1.9 m	10–16 02 2004	CCD SPEC	3360–7520	7.1	300B	600–900	QAP/DJF
MSSSO 2.3 m	12–14 06 2004	DBS B	3580–5520	2.8	600B	600–1200	QAP/MS
MSSSO 2.3 m	15–19 07 2004	DBS B/R	3870–5600; 6170–7110	2.5/1.2	600B/1200R	600–1200	DJF/AEV
SAAO 1.9 m	22–26 07 2004	CCD SPEC	3360–7520	7.1	300B	600–900	QAP/MS
UKST 1.2 m	11–20 08 2004	6DF V/R	3930–5600; 5310–7520	5.6/5.8	580V/425R	3 × 1800	QAP/AEJP
MSSSO 2.3 m	06–11 01 2005	DBS B/R	3680–5600; 6040–6950	2.5/1.5	600B/1200R	600–1200	DJF/QAP
MSSSO 2.3 m	10–14 07 2005	DBS B	3600–7400	4.5	300B	600–1200	DJF
MSSSO 2.3 m	19–25 05 2006	DBS B/R	3680–5600; 5480–7517	2.5/1.5	600B/600R	600–1800	QAP/BM

Notes: MSSSO 2.3-m telescope spectrograph slit generally set at 2.5 arcsec; SAAO 1.9-m spectrograph slit set at 2.4 arcsec; for the ESO 1.5 m, MSSSO 1.9 m and OHP 1.9 m the slits were set to 2.0 arcsec; FLAIR and 6DF fibres had an aperture of 6.7 arcsec.

(MOS) fibre systems (e.g. Peyaud et al. 2003, 2004). They permit 100–150 objects to be observed simultaneously over a 6° diameter UKST field. This affords substantial efficiency gains. A random montage of nine 6dF PNe spectra from the bulge fields is given in Fig. 3. Also note the contamination from a late-type star (or perhaps even a giant companion to the central star) in the bottom right-hand corner spectrum. Again this arises from time to time because the bulge fields are extremely crowded and the projected on-sky 6dF 100 μm fibre diameter is 6.7 arcsec.

The spectral reduction techniques employed depended on the telescope instrument combination. The FLAIR MOS fibre data were reduced using the IRAF 'dofibers' task whilst the more recent 6dF MOS fibre data were reduced using a special AAO package called 6DFDR which is a 6dF version of 2DFDR, the automated fibre reduction package developed for the 2DF MOS system on the AAT (e.g. Taylor et al. 1996). All the remaining SAAO and MSSSO observations were reduced using standard IRAF routines as reported previously in Parker & Morgan (2003).

A dedicated IRAF-based PN reduction package PNDR[4] was specifically developed by one of us (BM) to significantly improve the efficiency and versatility of the IRAF reductions, especially for the MSSSO observations. In many cases with FLAIR MOS data, both low and high dispersion spectral observations are available. In all such cases the high dispersion data are centred near the Hα line and these data are used wherever possible to derive the heliocentric systemic PN velocity and to estimate the nebular expansion velocity when the lines are well resolved. For the 6dF 2003 August and 2004 August observations, the separately reduced V and R spectra are joined into a single spectrum for ease of examination within the MASH data base though velocity determinations are based solely on the highest dispersion data. Sometimes there is a spectral discontinuity at this join which occurs at λ5610 Å.

4.1 Eliminating contaminants from the MASH catalogue

A wide range of different astrophysical objects have turned up in previous catalogues of PNe, mainly due to morphological similarity and/or detection of PN-like spectral signatures. This is often compounded by the associated poor imaging, low spectral resolution, inadequate wavelength coverage and/or insufficient signal-to-noise ratio (S/N) in the base discovery data. Kohoutek (1983) provides a good summary of PN mimics which includes H II regions, SNRs, reflection nebulosities, Wolf–Rayet (WR) shells, Herbig–Haro objects, symbiotic stars (and outflows) and low redshift emission-line

[4] Full details of the PNDR package, including a manual and the code, can be found at http://www.aao.gov.au/local/www/brent/pndr/.

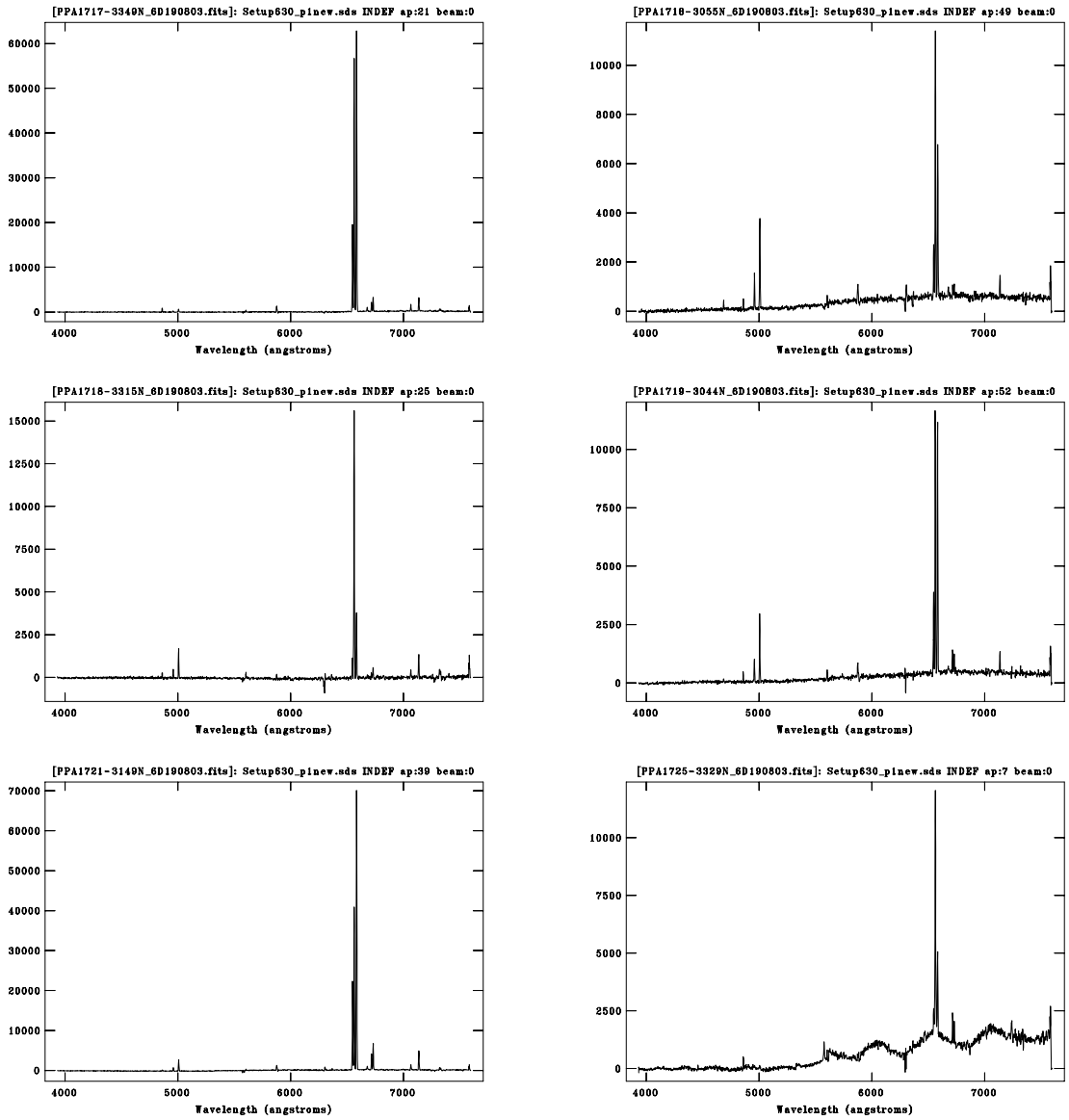

Figure 3. Montage of six random MASH bulge candidate PNe obtained with the AAO/UKST 6dF MOS fibre system in bulge survey field h630. These spectra are the result of splicing separate blue and red spectra taken with 580V and 425R volume phase holographic transmission gratings so the relative strengths of Hα and Hβ are no more than indicative. Note the contamination from an adjacent or perhaps even a companion late-type star to the PN central star in the bottom right-hand spectrum due to the large fibre diameters (6.7 arcsec) and very crowded fields.

galaxies. Stenholm & Acker (1987) and Acker & Stenholm (1990) identified 110 misclassified PNe in previous compilations based on a careful analysis of new optical spectra they obtained and the associated IRAS colours. We are keen to minimize such contamination in the MASH catalogue.

There is considerable overlap between SHS survey fields, so many candidate PNe are seen on more than one field, confirming their veracity and eliminating the possibility that they are emulsion flaws. Potential contamination from normal galaxies and reflection nebulosities are eliminated immediately via comparison with the matching contemporaneous broad-band SR exposures taken to accompany each Hα survey field. Their appearance remains almost identical between the two exposure types as the sampled flux in each band is mostly continuum. These 15-min SR exposures are well matched in depth to point source continuum objects such as stars in the 3 h Hα exposures, reaching to $R \simeq 20.5$ (Parker et al. 2005).

The great majority of H II regions are rejected on the basis of environment (i.e. in general star-forming regions) and morphology (i.e. irregular, interconnected shapes, dust-lanes, etc.) and stellar content. Ordinary faint nebulosities/Strömgren spheres around bright stars, although recognized as the likely identification by their proximity to these stars, are finally distinguished from chance line-of-sight projections via spectroscopy of the nebula and star and use of SuperCOSMOS photometry for the ionizing star to see if it is blue. Often apparently isolated nebulae found from initial visual scans of the Hα films are simply the brighter rims and concentrations of much more extensive nebula structures which are revealed when the SHS pixel data are examined under higher contrast. Most remaining contaminating H II regions, such as those that appear truly isolated and/or compact, are eliminated later from examination of the follow-up spectroscopy where for H II regions the [N II]/Hα ratio is generally less than 0.7 (e.g. Kennicutt et al. 2000). Objects

with higher ratios are usually either PNe, SNRs or Population I WR ejecta nebulae.

However, it is difficult to separate compact and/or isolated H II regions from very low excitation PNe (VLE PNe). As a caveat however, an unpublished slit spectrum of the peculiar high-latitude 'PN' PHL 932 shows strong Balmer lines, only weak [N II] and almost undetectable [O III] emission, and is practically indistinguishable from spectra of these aforementioned H II regions. Some of the MASH H II regions may therefore turn out to be 'PHL 932-type' objects and deserve further work. However, it is more likely that PHL 932 is not actually a PN but a Strömgren sphere in the ISM (Madsen & Frew, in preparation). Finally, we have checked the paper by Luo, Condon & Yin (2005) who cross-referenced an earlier version of the MASH catalogue (provided to them prior to publication) with NVSS radio data. This enabled a further number of contaminating H II regions to be removed based on what would be unreasonably strong radio flux for a PN at 1.4 GHz. Note that these remain as nominal PNe in their table 1.

Checking against Mid-course Space eXperiment (MSX) imagery (Price et al. 2001) can also be useful. The observations at 8 and 12 μm can reveal extensive, resolved material in photodissociation regions centred on or surrounding the optical nebula making a H II region identification likely. Alternatively, compact strong mid-infrared emission in all four MSX bands indicates a probable embedded star. Both cases make a PN identification unlikely (e.g. Cohen & Parker 2003).

The occasional Herbig–Haro object is removed on the basis of its spectrum (Cantó 1981), location in a star-forming environment, and either a jet and/or bow-shock morphology (e.g. Mader et al. 1999).

Population I WR nebulae (e.g. PCG 11; Cohen, Parker & Green 2005) generally have a brighter ionizing star relative to the nebula and are usually found close to star-forming regions. These WR nebulae, arising from either wind-blown shells or processed ejecta, can often mimic PN morphologies and can also have similar optical emission-line ratios. However, WR nebulae usually have a low galactic latitude and are dusty, making them strong mid-infrared sources.

Galactic SNRs, including several new SHS based discoveries (e.g. Parker, Frew & Stupar 2004; Stupar et al. 2006), are often initially identified by their filamentary morphology and positional coincidence with a non-thermal radio source. The detection of strong [S II], [O II] and [OI] emission lines in follow-up spectroscopy, when combined with indicative diagnostic line ratios (Fesen, Blair & Kirshner 1985), confirms their SNR nature.

Of more utility as a discriminant between the above contaminants and PNe is a diagnostic diagram using both [N II] and [S II] line strengths (e.g. Sabbadin & D'Odorico 1976; Sabbadin, Minello & Bianchini 1977; Cantó 1981). An updated version using PN data from Acker et al. (1992) is presented by Riesgo-Tirado & López (2002; their fig. 1). However, the [N II]/Hα ratio alone must be used with caution as most higher excitation PNe have relatively weak [N II] emission. Indeed, very high-excitation PNe (e.g. Kaler 1981), including many in MASH, have no measurable [N II] or [S II] emission. If only red spectra are available for such an object, then other criteria (morphology, central star, environment, etc.) will be needed to classify it unambiguously.

As an example of an identification problem, a number of large, nearby (currently accepted) PNe may in fact be Strömgren spheres in the ISM ionized by a hot pre-white dwarf or subdwarf (the original PN having long since dissipated). These may have line ratios which mimic true PNe; for example, Hewett 1 (Hewett et al. 2003) has been shown by Chu et al. (2004) to perhaps not be a bona fide PN. DeHt 5, Sh 2-174, and RE J1738+665 may also be examples of such cases. Their true nature is currently being investigated by Madsen & Frew (in preparation).

A further area of concern with contamination is in the Galactic bulge. Many bulge emission sources are compact or even unresolved and spectra alone can sometimes be insufficient if S/N and wavelength coverage are inadequate and ancillary information in terms of MSX imagery and two-Micron All-Sky Survey (2MASS) colours, for example, are inconclusive. Several unusual point source emitters have been discovered and they will form the basis of separate publication(s).

Symbiotic stars (e.g. Belczyński et al. 2000) are one likely source of remaining contaminants. Several probable symbiotics have already been removed from the MASH data base based on red DENIS IJK_s and/or 2MASS JHK_s colour indices (Schmeja & Kimeswenger 2001; Larios & Phillips 2005), evidence for a red continuum in the optical spectrum, or strong [O III]λ4363 emission relative to Hγ (see Gutiérrez-Moreno, Moreno & Cortés 1995). Even so, it is probable that a number of symbiotic stars remain in the catalogue due to poor S/N preventing detection of the fainter diagnostic lines, especially if heavily reddened. Previous PN catalogues almost certainly retain symbiotic contaminants for the same reasons though several were removed from the Acker et al. catalogues by Mikolajewska, Acker & Stenholm (1997). Furthermore, several extreme bipolar objects (e.g. PHR1253−6350) in the catalogue may be objects similar to resolved symbiotic outflows typified by He 2-25, He 2-104 and BI Cru (Corradi & Schwarz 1993; Corradi 1995; Corradi et al. 1999). These are qualified as only possible PNe in the data base for the time being.

Finally, any resolved nebulae with questionable morphology and which are rejected as PNe on the basis of these diverse comparisons and/or the lack of adequate S/N spectra are retained in a different file if they are not already recorded as an optical nebulosity in SIMBAD. These will form the basis of a separate publication as the 'miscellaneous emission nebulae' or 'MEN' catalogue (Parker et al., in preparation). This currently has about 400 entries and is of considerable scientific interest in its own right. Some of these nebulae may eventually return to the MASH catalogue when deeper spectroscopic and photometric information become available.

In summary, the majority of PNe discovered are discrete sources with classic PN-type morphologies and associated PN-type spectral signatures. Occasionally, neither the candidate morphology or spectroscopy are sufficiently conclusive to merit a definite PN designation. This is especially true of those that are more extended and/or that show evidence of interaction with the ISM. In the absence of other supporting information (e.g. identification of a central star, hereafter CSPN) such candidates are recorded as possible PNe in the data base. Only six contaminating emission-line galaxies have been found from follow-up spectroscopy and these were relatively nearby with active star formation which therefore stand out in the Hα bandpass. The gas velocity has to be sufficiently low ($\leqslant$1200 km s^{-1}) to fall within the 70 Å bandpass of the interference filter. None of these were previously known. Conversely, the MASH catalogue also contains 11 PNe which had been previously identified as galaxies, usually based on searches for isolated diffuse objects in Galactic plane 'zone of avoidance studies' from broad-band photometry.

5 MASH ONLINE CATALOGUE DESCRIPTION AND ACCESS

The data base was constructed by QAP and checked by QAP/DJF/AA and then cross-checked and ported by FO into

standard Centre de Données astronomiques de Strasbourg (CDS) formats for general SIMBAD/VizieR accessibility (Ochsenbein, Bauer & Marcout 2000). It takes the general form of a simple table of numbers and character values with clickable links to the FITS images and spectra for each PN and a more detailed summary page for each object. The structure is similar to the preliminary version released on CD-ROM in 2001 (Parker et al. 2001, 2003) but now presented in the standard VizieR way for online catalogues for straightforward access and manipulation/query. The CDS[5] has accepted responsibility for maintaining the MASH catalogue data products via liaison between QAP and AA/FO. For convenience, both the SHS Hα and SR image data for all the MASH PNe, plus the preliminary 1D reduced spectra, are available to download as part of the online MASH catalogue. MASH is available from http://vizier.u-strasbg.fr/vizier/MASH.

When the MASH data base is accessed via VizieR an introductory page is first presented which contains a brief description of MASH followed by several useful links to the main MASH catalogue, spectra, gallery of images and to this paper. The first clickable link is to the main MASH catalogue V/127/mash, which brings up a standard VizieR interface to the catalogue where available columns can be selected for retrieval or where selections according to column values can be made. For the current release there are 19 columns but this will increase when other parameters such as radial velocity, emission-line ratios, etc. are added. Only a subsection of these columns are available by default. A VizieR data base page of a selection of key column entries from the MASH catalogue is presented in Fig. 4. The second clickable option brings up direct access to the reduced 1D spectra of each MASH PN which can be viewed, expanded, saved as a postscript file, viewed as an ASCII table or downloaded directly as a FITS file (of course access to the spectra is also available from within the main catalogue). Note many MASH PN have more than one available spectrum. The third clickable link brings up the MASH image gallery of individual PN images in colour (created by combining the SHS Hα and SR images with the SuperCOSMOS B_j image). Each colour image is also a clickable link which brings up the standard summary page for each PN also available form the main MASH catalogue (Fig. 5).

MASH is still an evolving entity where planned updates will be released in stages to incorporate important new parameters for each PN as they are compiled together with any additional MASH PNe uncovered. However, it was felt important and timely, especially given the interval since the preliminary CD-ROM, to release the MASH catalogue to the community now that individual PN veracity has been carefully checked, accurate positions and sizes obtained and confirmatory spectra reduced. Another important difference between MASH and the earlier version is that the catalogue now contains only new PNe for which we claim first or independent discovery. All objects previously identified as *true* PNe by others have been removed. MASH does though include some PNe that have been susbsequently rediscovered or independently found by others after our original discovery, confirmation and release on our original CD-ROM in 2001 (e.g. the small samples in Kohoutek 2002 and Boumis et al. 2003, 2006) as well as 64 objects whose identity as a PN was uncertain until new MASH imagery and spectroscopy were obtained.

The Hα and matching red images downloaded from the SHS web site for each PN are provided via a direct link within the VizeR MASH summary page for each PN as FITS files with comprehensive header information which details key photographic, photometric, astrometric and scanning parameters (e.g. Hambly, Irwin & MacGillivray 2001b). The default size of the extracted image areas is 4×4 arcmin^2 which is sufficient to adequately view all but the most extended MASH PNe. The $\sim$35 PNe with major axes larger than 4 arcmin are mostly available as 15×15 arcmin^2 images. Exceptions are PFP1, FP0905$-$3033 and FP1824$-$0319, which are 15–30 arcmin across. In these and a few other cases the relevant area from the 16$\times$ blocked FITS data is used. The FITS images also have an accurate built-in world coordinate system (WCS) as well as a FITS table extension that contains the IAM image parameters (e.g. coordinates, sizes, magnitudes, orientations and shapes) for every object detected in the image area (e.g. Beard, MacGillivray & Thanisch 1990). This permits the photometry of any CSPN candidate to be checked and its accurate position used directly. This also facilitates easy incorporation of the data into other software packages such as the Starlink GAIA environment for subsequent visualization, investigation, manipulation and comparison with other data.

5.1 The main MASH online data base description and column entries

Access to individual MASH PN summary page: M

There is a clickable icon near the front of each record with column ID 'M'. This brings up a separate summary page for each PN which presents a colour composite image of the PN (created from the Hα (red channel), SR (green channel) and B_j (blue channel) SuperCOSMOS 4×4-arcmin^2 survey images) together with the individual SR, Hα and reduced 1D spectral images and other pertinent details.

Object status flag: n_PNG

This is given as T, L or P where

T indicates a true confirmed PN discovery with indicative morphology, spectral features and sometimes an obvious CSPN.

L indicates an object which is likely to be a PN but whose imagery or spectroscopy are not completely conclusive.

P indicates a possible PN. The morphology and spectroscopy are insufficiently conclusive, usually due to a combination of low S/N spectra, insufficient wavelength coverage, very low surface brightness or indistinct nebulosity. Recall that the vast majority of contaminating H II regions, SNRs, HH objects, etc. have already been removed and saved in the associated 'miscellaneous emission nebulae' catalogue.

Standard IAU PN G designation as lll.l±bb.b: PNG

This follows the currently accepted IAU convention for Galactic PNe which cuts the determined l, b values to 0.1 and so allows up to 0.1 error (e.g. PN G349.9+03.2).

Usual name, for example, PHR/PPA/FP designation: NAME

As well as the IAU PN designation we assign a unique catalogue identifier for each new discovery. The nomenclature (also used on the preliminary 2001 CD-ROM) follows from the first character of the prime discoverer's surname. The name stem PHR (Parker, Hartley, Russeil) is used for the main 751 MASH discoveries, followed by PPA (Peyaud, Parker, Acker) for the 137 new bulge PNe discovered from difference imaging of the SHS data and finally FP (Frew, Parker) for 14 new, large, evolved PNe mainly from the blocked-down FITS images. There then follows a concatenation of the J2000 equatorial coordinates of right ascension

[5] http://cdsweb.u-strasbg.fr/

(RA) hours and minutes and the declination (Dec.) degrees and minutes (e.g. PHR1706−3528). There are four exceptions to the usual names. One is the extremely large 30 arcmin diameter PN PFP1 (Pierce et al. 2004). There is then a single entry with an HP (Hopewell, Parker) designation which refers to a compact PN discovered during a 6dF spectroscopic follow-up run for emission-line star candidates and finally two PNe confirmed at SAAO by Retha Pretorius for a similar programme. These have PKP (Pretorius, Knigge, Parker) designation. These last three compact PNe were identified from the SHS IAM data on the basis of their Hα excess.

J2000 equatorial coordinate positions for the new PN: RAJ2000, DEJ2000

The precise J2000 RA/Dec. coordinates determined for each new PN are generally good to ∼1–2 arcsec depending on the visible extent of the PN. Where an obvious CSPN is visible in SHS data the accurate stellar position, as given by the IAM data, is the value adopted. In most cases, due to the faintness and angular extent of the new PNe and the red bandpasses of the Hα and SR images, the CSPN are beyond the limit of detectability in the SHS data (refer Figs 1 and 2).

In the absence of a positive CSPN identification, the geometric centroid of the nebula, as seen in Hα light, was determined. Most PNe are fairly compact so this measurement is quite straightforward. Further work to identify CSPN candidates has commenced and we present our preliminary findings in Section 7.

The positional accuracy decreases for large, extended or asymmetric candidates where, in the absence of a clearly identified CSPN, a subjective assessment is made as to the geometric centre of the object. For some highly evolved PNe the CSPN can be offset from the geometric centre of the nebula by tens of arcseconds due to proper motion between the star and ejecta (e.g. Tweedy & Napiwotzki 1994; Tweedy, Martos & Noriega-Crespo 1995). The correct position to use for the object then becomes problematic and dual coordinates may be required. As a simple test we undertook a comparison between our determinations and published positions for 54 known PNe as recorded in Acker et al. (1992, 1996). The sample was retrieved via SIMBAD from a 6–9 h RA zone which contains a range of objects whose angular sizes vary between 17 and 210 arcsec. We find a median positional difference of 2.0 arcsec and a dispersion of 5 arcsec with the difference larger for more extended PNe as might be expected. The comparison used remeasured positions for all the known PNe from the DSS images undertaken by I. Lundström in 2001 (see Ochsenbein et al., in preparation).

Kimeswenger (2001), Kohoutek & Kühl (2002) and Kerber et al. (2003) have also independently remeasured the positions of all known PNe from DSS images in an attempt to provide improved coordinates. We are able to undertake the same measurements but using the more appropriate SHS Hα images which have an in-built accurate WCS. These often reveal outer extensions and asymmetries which could affect estimates of PNe position in the absence of a CSPN identification. Hence, both previously known and MASH PNe can be placed on exactly the same astrometric grid and waveband. These Hα based uniform coordinates, together with new dimension estimates and notes on additional faint extensions for all previously known PNe in the SHS survey area, will be published separately.

Galactic longitude and latitude: GLon, GLat

These are calculated directly from the derived J2000 coordinates and quoted to three decimal places.

Measured angular extent: Major and Minor axes: MAJDiam, MINDiam

These are given in two columns as major and minor axis (in arcsec) as directly measured from the SHS digital Hα images. For a few (<15) highly asymmetric PNe only the major axis is defined. The measured values represent an estimate of the best *visible* size of the images as seen in Hα plus [N II] light to the nearest arcsecond, and including evident crowns or extended discs but not any extremely faint haloes (if visible these are mentioned in the accompanying notes). The accuracy of these measures depends on the morphological clarity of the PN, with outer boundaries being harder to determine for more diffuse candidates. An attempt was made to measure all dimensions at the same 98 per cent contrast level using facilities within the Starlink GAIA package which allow direct on-image dimension estimates. Clearly this process is somewhat subjective but careful attempts have been made to undertake this task uniformly.

Morphological classification: Morph

A detailed description of the morphological classifications applied to the sample and some of the subsequent analysis form the basis of a separate paper (Parker et al., in preparation). However, after review of the variety of extant schemes previously developed, an adaptation of the current Corradi & Schwarz (1995) classification was employed, based in turn on that developed by Schwarz, Corradi & Stanghellini (1993). We use a basic 'ERBIAS' classifier to indicate PNe which are Elliptical (oval), Round, Bipolar, Irregular, Asymmetric or quasi-Stellar (point source). We make the added distinction between elliptical and purely round PNe on the basis of interest in these particular canonical Strömgren spheres (e.g. Soker 2002) where an object is considered to be Round (circular) if the difference between estimated major and minor axis is <5 per cent. In uncertain cases a dual classification might be applied such as E/B.

We then add a subclassifier 'amprs' which indicates that the main object has a one sided enhancement/asymmetry 'a', has multiple shells or external structure 'm', exhibits point symmetry 'p', has a well defined ring structure or annulus 'r' or resolved internal structure 's'. A morphological classification should normally have only one basic 'ERBIAS' classifier but can have several 'amprs' subclassifications as the image resolution and clarity allows and ordered alphabetically.

An example montage of new PNe exhibiting these morphological classifications is given in Fig. 6. In Table 2 we present the morphological results from MASH PNe We have so far found only ∼50 very compact 'star-like' PNe mostly in the core bulge region where difference imaging proved effective since MASH discoveries are largely from visual scanning which is largely insensitive to compact (star-like) emitters. Also with PNe image sizes below about 10 arcsec the assigned morphological classification are provisional until the advent of higher resolution imaging. We are now in the process of trawling the online SHS data for compact PNe.

Follow-up spectroscopy: telescopes used: TEL and dates of observation: Obs

A variety of different 2-m class telescopes were used to perform the follow-up optical spectroscopy of the MASH PNe candidates during 30 observing missions between 1998 and 2005. The first column is a two character key denoting the telescope used: M1: MSSSO 1.9 m; MS: MSSSO 2.3 m; SA: SAAO 1.9 m; OH: OHP 1.9 m; FL: FLAIR MOS system on UKST; 6D: 6dF MOS system on UKST; E1: ESO 1.5m. The raw-count spectral 1D FITS images will be replaced by the flux-calibrated 1D FITS spectra in a future MASH release. The spectral observation date is expressed as

M	n	PNG	Name	RAJ2000 "h:m:s"	DEJ2000 "d:m:s"	GLon deg	GLat deg	MajDiam arcsec	MinDiam arcsec	Morph	Tel	Obs "Y:M:D"	HaExp	HaFld
	T	G209.1-08.2	PHR0615-0025	06 15 20.4	-00 25 49	209.1757	-8.2227	100.0	100.0	R	MS	2005-01-07	HA19062	HA1285
	P	G227.3-12.0	PHR0633-1808	06 33 24.9	-18 08 23	227.3207	-12.0289	17.0	15.0	Ea	SA	2003-02-02	HA18191	HA926
	T	G212.2-04.7	PHR0633-0135	06 33 09.3	-01 35 12	212.2603	-4.7910	56.0	50.0	Ea	SA	2004-02-16	HA19062	HA1285
	P	G214.2-02.4	PHR0645-0217	06 45 03.5	-02 17 52	214.2511	-2.4663	55.5	46.0	Es	SA	2003-01-29	HA18685	HA1196
	L	G223.6-06.8	PHR0646-1235	06 46 25.4	-12 35 56	223.6338	-6.8035	40.0	37.0	E	SA	2006-02-22	HA18194	HA1016
	L	G219.1-03.9	PHR0648-0719	06 48 43.8	-07 19 51	219.1592	-3.9343	35.0	33.0	Ea	SA	2000-02-08	HA18693	HA1107
	T	G212.6-00.0	PHR0650+0013	06 50 40.5	+00 13 40	212.6422	-0.0659	68.0	26.0	B	SA	2004-02-13	HA19075	HA1286
	T	G215.5-01.4	PHR0651-0257	06 51 07.2	-02 57 07	215.5234	-1.4162	8.5	8.5	R	SA	1999-01-13	HA17887	HA1197
	P	G221.8-04.2	PHR0652-0951	06 52 19.4	-09 51 36	221.8238	-4.2837	60.0	46.0	Ea	SA	2003-01-30	HA18693	HA1107
	P	G224.3-05.5	PHR0652-1240	06 52 20.3	-12 40 34	224.3504	-5.5463	187.0	180.0	I	SA	2003-01-31	HA18244	HA1017
	T	G222.8-04.2	PHR0654-1045	06 54 13.4	-10 45 38	222.8412	-4.2730	27.0	16.0	E	SA	2003-01-28	HA18244	HA1017
	T	G224.3-03.4	PHR0700-1144	07 00 05.8	-11 43 51	224.3616	-3.4280	49.0	47.0	Ea	SA	2003-01-29	HA18244	HA1017
	L	G221.0-01.4	PHR0701-0749	07 01 09.3	-07 49 21	220.9984	-1.4147	67.0	66.0	Ea	SA	2003-01-28	HA18693	HA1107
	T	G217.2+00.9	PHR0702-0324	07 02 34.2	-03 24 35	217.2356	0.9177	52.0	44.5	Ea	SA	1999-01-13	HA17887	HA1197
	T	G214.6+02.9	PHR0704-0011	07 04 56.6	-00 11 15	214.6399	2.9189	14.0	14.0	R	SA	2004-02-13	HA19046	HA1288
	T	G227.2-03.4	PHR0705-1419	07 05 38.5	-14 19 05	227.2852	-3.4029	15.0	15.0	E	SA	2003-01-29	HA18244	HA1017
	T	G222.9-01.1	PHR0705-0924	07 05 51.4	-09 24 11	222.9361	-1.1056	85.0	80.0	B	SA	2003-01-28	HA18693	HA1107
	P	G237.9-07.2	FP0711-2531	07 11 32.0	-25 31 24	237.9490	-7.2470	660.0	600.0	Ea	SA	2004-02-14	HA19099	HA756
	T	G226.4-01.3	PHR0711-1238	07 11 43.3	-12 38 03	226.4677	-1.3165	56.5	55.0	Ra	SA	2003-01-29	HA18263	HA1018
	L	G225.2+00.1	PHR0714-1051	07 14 28.8	-10 51 44	225.2104	0.1031	7.0	5.0	E	MS	2005-01-07	HA18263	HA1018
	T	G225.4+00.4	PHR0716-1053	07 16 08.0	-10 53 06	225.4195	0.4518	104.5	71.0	Em	SA	2000-02-08	HA18263	HA1018
	T	G227.1+00.5	PHR0719-1222	07 19 46.7	-12 22 47	227.1581	0.5422	193.0	188.0	Ea	SA	2000-02-08	HA18263	HA1018
	P	G215.0+07.4	FP0721+0133	07 21 41.0	+01 33 31	214.9990	7.4390	720.0	720.0	A	SA	2004-02-14	HA19046	HA1288
	T	G238.1-04.6	PHR0722-2431	07 22 14.3	-24 31 02	238.1645	-4.6301	21.0	20.0	R	SA	2003-01-28	HA19352	HA757
	T	G229.3+00.0	PHR0722-1434	07 22 14.9	-14 34 49	229.3826	0.0376	93.0	60.0	Es	MS	2005-01-08	HA18256	HA928
	T	G222.1+03.9	PFP1	07 22 17.7	-06 21 46	222.1292	3.9104	1150.0	1100.0	Ra	SA	2004-02-13	HA18771	HA1109
	P	G228.1+00.8	PHR0722-1305	07 22 30.6	-13 05 30	228.0997	0.7954	44.5	20.5	R?	MS	2005-01-08	HA18282	HA1019

Figure 4. Selection of the key column entries from the MASH online catalogue (list in RA order).

year-month-day of the *first* spectroscopic observation made to confirm the MASH PN candidate.

UKST Hα survey exposure and survey field number: HAExp, HAFld
These two values simply record the original Hα survey field exposure number and official survey field number on which each PN was originally found. Note that due to the considerable overlap between SHS survey fields some PNe are visible on up to four different survey fields. Furthermore, some fields, especially those in the bulge, may have dozens of new PNe identified.

Number of available spectra of each MASH PN: Nsp
Many MASH PNe have several spectroscopic observations on the same or different telescopes. Hence we have a variable 'Nsp' whose value ranges for 0–7 and gives the number of reduced 1D FITS spectra available to view/download by cliking this Nsp link. The most recent available spectrum is presented by default on the summary page for each MASH PN. Note, although we have obtained 100 per cent spectral coverage for MASH there may temporarily remain a few PNe for which spectra are not yet available to download.

Comments
The comments accompanying each record are a heterogeneous set of remarks concerning each PN, including details of repeat spectroscopic observations, morphological oddities, basic line ratio comments and whether the PN also has a WR CSPN. If the PN was previously identified as another object or designated as only a possible PN in SIMBAD the previous ID and reference is also given.

5.2 Planned updates to catalogue entries

The flux calibrated spectra are currently being used to derive line ratios (AA/QAP/DJF) and will, where possible, be used to determine reddenings, excitation classes, nebular abundances, densities and temperatures using the HOPPLA code (e.g. Köppen, Acker & Stenholm 1991). These results will be presented in a future series of papers and incorporated into subsequent releases of the MASH catalogue. Note that further columns will be added to later online catalogue releases to incorporate such line ratios, radial and expansion velocities, integrated Hα nebular fluxes and other information as it is determined.

6 BASIC PROPERTIES OF THE MASH SAMPLE

MASH has simultaneously explored a new, low surface brightness region of PN discovery space and detected significant numbers of compact but faint (distant) PNe in the Galactic bulge. MASH has increased by ∼60 per cent the number of Galactic PNe accrued from all sources over the last 75 yr (e.g. compared with the 1510 total PNe recorded in Kohoutek 2001 and 1385 true and probable PNe in Acker et al. 1992, 1996). This is a critical contribution that will facilitate our understanding of the initial and terminal phases of PNe life by preferentially offering for study a higher fraction of young compact or large, highly evolved objects.

MASH has essentially the same fraction of bipolars as among previous samples. Corradi & Schwarz (1995) found 14 per cent of a sample of 400 PNe to have a bipolar morphology, while Manchado (2004) found 17 per cent from 255 PNe. From our complete new sample of 905 PNe we find that 114 (12.5 per cent) are classified as bipolar or possible bipolar nebulae. If we restrict the selection to PNe in the RA range 6–17.5 h, thus avoiding the bulge, this fraction rises to 15 per cent. We independently confirm, for the completely new MASH sample, the trend that bipolar PNe are restricted to lower

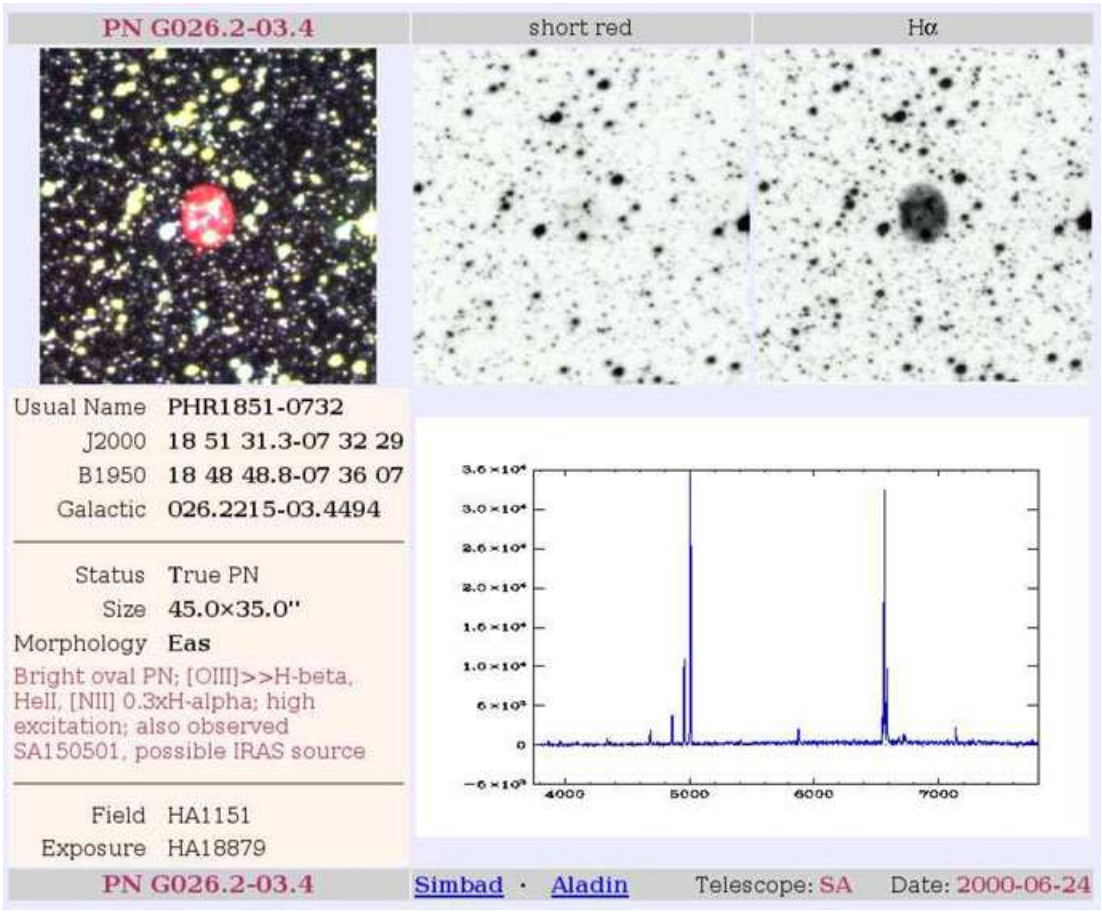

Figure 5. Example of an individual PN summary page from the MASH online catalogue. Top: Hα/SR/B combined colour image, SR and Hα images of size 4×4 arcmin; Bottom: summary information and 1D spectrum.

average galactic latitudes and therefore scaleheights (e.g. Corradi & Schwarz 1995) as shown in Table 2. We find about a 1° reduction in $|b|$ compared to all the other types.

Soker (1997) explored the relationship between PNe morphology and binary progenitors characterizing the evolutionary roots of 458 Galactic PNe according to his classifications of their shapes. The arcsecond resolution of MASH provides decent morphological detail, revealing both inner and outer structures of PNe, enabling us to test such evolutionary theories of PNe formation and shaping from a comprehensive and self-consistent sample. Further details of the morphological analysis of the MASH sample will be given by Parker et al. (in preparation).

A large fraction of our sample are of very low surface brightness. The average nebular major axis dimension is 51 arcsec with a median of 22 arcsec, but with some objects extending to several arcminutes (refer bottom left-hand panel in Fig. 7. Our largest MASH PN is nearly 30 arcmin across: FP 1824−0319. This compares with an average size of <10 arcsec for PNe in the Acker et al. (1992, 1996) catalogues. This indicates that many of our sample are in a highly evolved state and/or local, where the central star has faded from easy optical detection and the nebula itself is dissolving into the ambient ISM. MASH also reveals additional nebular features such as external haloes, jets and blobs around many known PNe. This may itself have significant implications for previous derived PNe properties such as distance and total ejecta mass estimates (e.g. Parker 2000, for NGC 2899).

A few basic plots of the new data are provided in Fig. 7. The top two plots show the galactic latitude histograms of the Acker et al. (1992) and MASH catalogues, respectively, but restricted to a $|b|$ of 15° (the MASH limit dictated by the SHS coverage). The surface density of known PNe in Acker falls off sharply near Galactic latitude $b = 0°$ due to extinction but new MASH PNe are found much closer to $b = 0°$ than previous samples, as can be seen (greater PN numbers at low $|b|$ and a narrower low $|b|$ deficiency gap), especially away from the heavily obscured bulge region. This improved low latitude coverage is testimony to the survey's excellent sensitivity in the narrow red Hα band which is also less affected by dust than [O III] images (see top left-hand panel in Fig. 7).

The middle two plots of Fig. 7 gives the Acker et al. (1992) (left-hand panel) and MASH (right-hand panel) Galactic latitude versus longitude distributions for PNe in the region of overlap of both samples in the southern Galactic plane. These clearly show the strong PN number density enhancement of the MASH sample in the bulge region and a more uniform bulge and disc distribution compared to the equivalent Acker sample plot.

The final two plots give the MASH histograms of galactic longitude (bottom left-hand panel) in and major axis dimensions (bottom right-hand panel). The strong concentration to the Galactic Centre is clear as is the slow decline outside of the sharp drop off at ±10°. The distribution of major axis diameters has a much longer tail to larger angular size compared to that in Acker. Note there is no overlap in the contents of either catalogue.

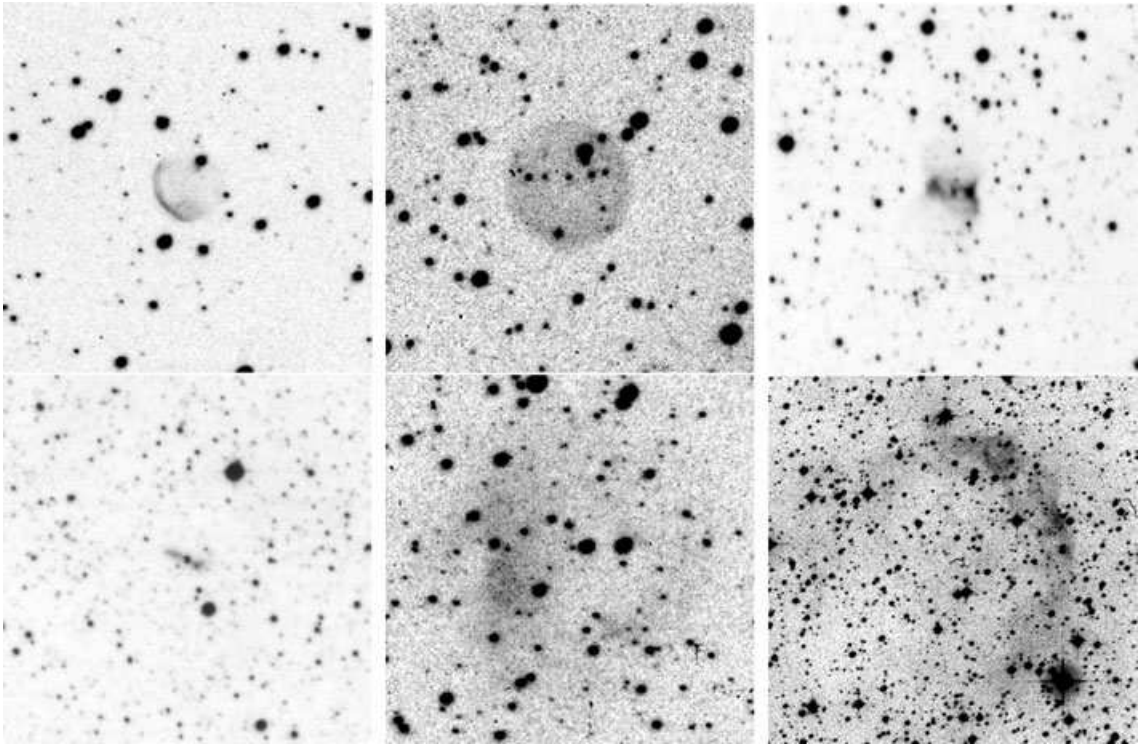

Figure 6. Extracts of SHS data around six newly discovered MASH PNe illustrating the basic morphological types. Top left-hand column: Ea elliptical with asymmetric enhancement (PHR0700−1143); top middle column: R – round (PHR0843−2514); top right-hand column: Bs – bipolar with resolved internal structure (PHR1408−6229); bottom left-hand column: B – extreme bipolar/possible symbiotic outflow candidate (PHR1253−6350); bottom middle column: Is – irregular shaped PN with some internal structure (PHR0652−1240); bottom right-hand column: As – asymmetric PN, again with some structure (PHR0743−1951). The first five images are 4 × 4 arcmin^2 and the bottom right-hand column is 10 × 10 arcmin^2 in size.

Table 2. Summary details of morphological classifications for all 903 new MASH PNe.

Class	Total number	Per cent fraction	$\langle\|b\|\rangle$	σ	$n > 10$ arcsec
E: elliptical	492	54.4	3.50	2.39	432
R: round	175	19.3	4.05	2.51	146
B: bipolar	113	12.5	2.51	1.84	109
I: irregular	39	4.3	3.23	2.02	39
A: asymmetric	36	4.0	3.44	2.80	36
S: star-like	50	5.5	3.03	2.31	0

Note that at RAs greater than $17^{\rm h}30^{\rm m}$ the bulge increasingly dominates and a larger fraction of MASH PNe are compact making precise classification difficult, especially for objects <10 arcsec in diameter. There has been no pre-selection of this list into true, likely and possible PNe. The average $|b|$ values in degrees for each type are for PNe with major axes diameters >10 arcsec except for those of type S. The bipolar group contains 32 PN that are only possible bipolars.

Detailed statistical analysis of the MASH sample will be presented in future papers in the series.

7 IDENTIFICATION OF CENTRAL STARS

Preliminary work to identify CSPN candidates has commenced using both the SSS and SHS data. Each PN in the MASH catalogue was subjected to quotient imaging. 4-arcmin^2 quotient images around each PN were created from the broad-band SuperCOSMOS B_J (blue) and equivalent R_F (red) images in an attempt to identify any clearly blue CSPN. These were inspected along with the equivalent B_J, R_F, Hα and SR images and then manually blinked to try to identify any possible CSPN within the photometric limits of each bandpass. Initially quotient B_J/R_F images were used, but these were often found to suffer from broad-band nebular contamination in the R_F image for bright PNe. This was overcome by utilizing the shorter exposure *SR* data. Image subtraction was also used to supplement our analysis.

Although no PSF matching of the data were undertaken prior to division or subtraction, the technique is surprisingly effective at isolating blue stars (Fig. 8). Hence, a large number of new CSPN candidates have been found and will be incorporated into subsequent MASH releases. However, the inherent faintness of many central stars and the limiting depth and resolution of the SuperCOSMOS SSS and SHS data restricts the numbers of true CSPN that can be identified in this way. Nevertheless, from our preliminary analysis we estimate that ∼30 per cent of the MASH entries have candidate

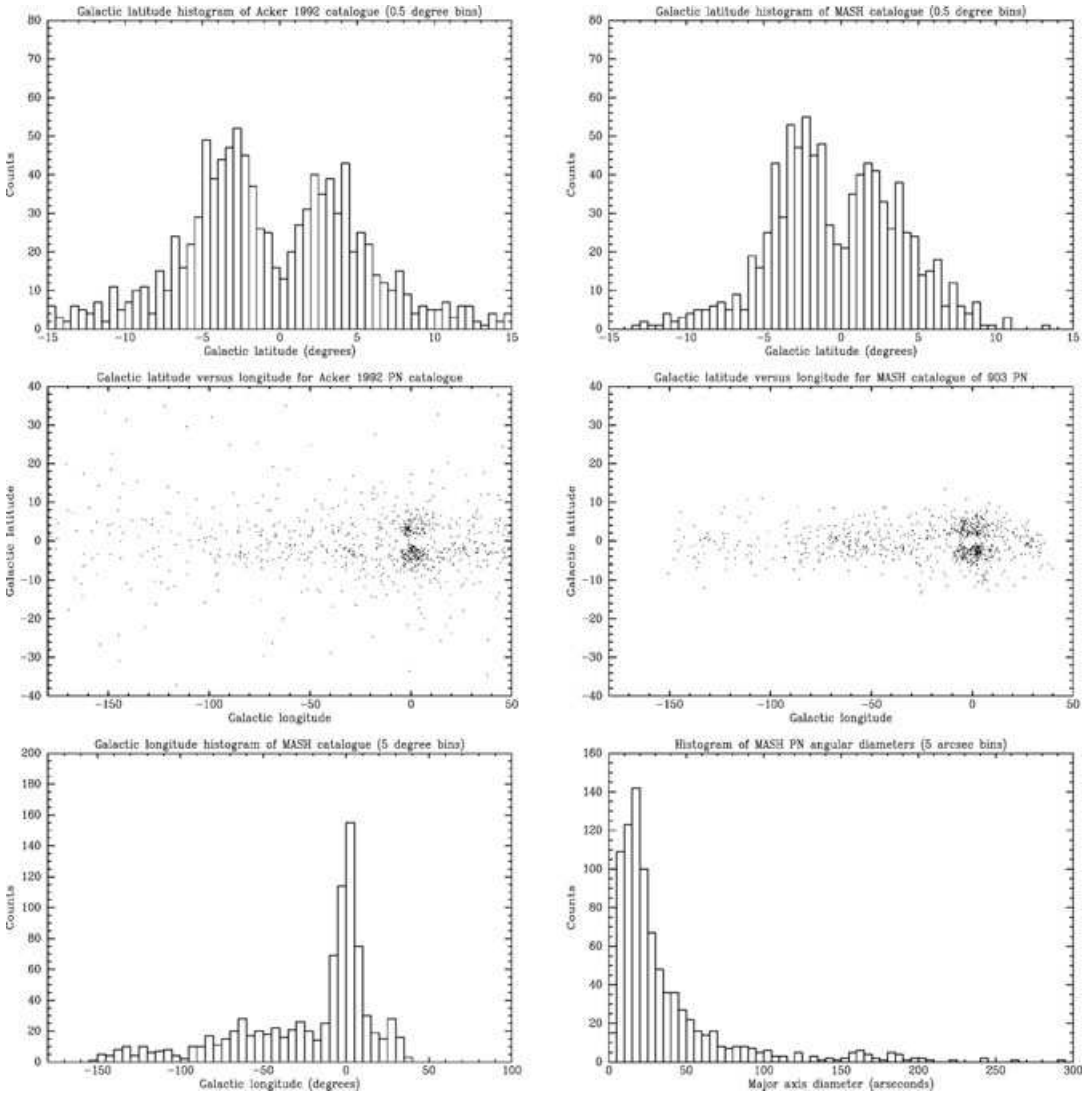

Figure 7. Basic plots of the comparison between the Acker catalogue and new MASH PNe. The top two plots show the galactic latitude histograms of the Acker and MASH catalogues, respectively. The middle two plots show the galactic latitude versus longitude plots of the Acker and MASH PN in the region of overlap in the southern galactic plane. The final two plots give the MASH histograms of galactic longitude in degrees and major axis dimension in arcsec. Note that there is no overlap in the contents of the Acker and MASH catalogues.

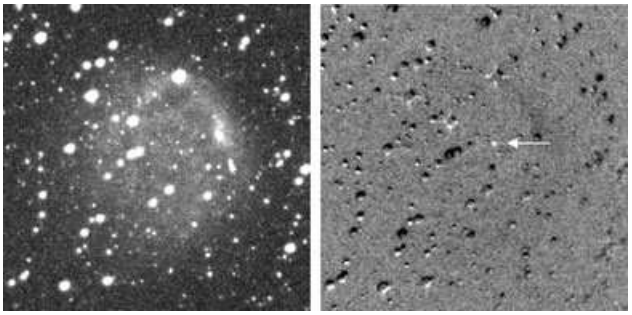

Figure 8. Identification of the central star candidate of PHR0942−5220 with Hα (left-hand panel) and $B_J - R_F$ difference (right-hand panel) images shown here. Notice the off-centre position of the central star $B_J = 19.8$) as indicated.

CSPN, with about half of these representing high quality candidates suitable for immediate follow-up.

We have also begun to extract photometric information from the associated SuperCOSMOS IAM data for these candidates. The vast majority of decent CSPN candidates have $B_J \geqslant 18$. The photometric accuracy of the SuperCOSMOS data is limited to ± 0.15 mag (Hambly et al. 2001b), but this can be considerably larger in the galactic plane due to image crowding and nebular contamination. Although the resolution of the SuperCOSMOS data has prohibited proper deblending of some CSPN candidates, we plan to address this using SEXTRACTOR. This photometric data will be superseded by an ongoing programme of follow-up *UBVRI* photometry. Positions and magnitudes for identified CSPN will be incorporated into subsequent updates to the MASH catalogue.

8 CURRENT MASH PROJECTS

Several projects underway by the MASH team will result in major catalogue updates over the next two years. The current MASH

catalogue largely contains well-resolved PNe because of the search techniques originally employed before the availability of the online digital SHS data in 2002. These visual scans were not particularly sensitive to compact/barely resolved emitters. However, ∼30 per cent of PNe in previous catalogues have angular size ⩽6 arcsec, so large numbers of faint point source/barely resolved candidates can be expected to be discovered from our survey when large-scale difference imaging is performed. This will be especially true away from the rich bulge fields which we have already extensively investigated via this method. Difference imaging works well because the Hα and SR data PSFs are very similar (e.g. same telescope, emulsion and point source depth). For other projects, point source emitter candidates are selected from the SuperCOSMOS IAM data (and not the pixel data), using a combination of H$\alpha - R$ versus $R - I$ colour–colour plots. Several compact PN candidates have already been found in this way (Pierce 2005).

We also plan to determine accurate, integrated Hα fluxes for all well-resolved MASH PNe using the SHS survey calibration to a Rayleigh scale made possible through direct comparisons with the Southern Hα Sky Survey Atlas (SHASSA) of Gaustad et al. (2001). SHASSA provides calibrated narrow-band (Hα + [NII]) and continuum images of the entire southern sky. The calibration process is described by Pierce et al. (2004) and Frew & Parker (in preparation). Our available spectroscopy permits a deconvolution of the [NII] contribution to the SHS Hα image (although we have to assume that this ratio remains effectively constant across the PN). In a further paper in this series we will present integrated Hα fluxes for MASH PNe wherever possible.

A more general brief description of current work is given below.

8.1 Evolved PNe

The most highly evolved PNe are the major component of any volume-limited sample as they numerically dominate the luminosity function. Such PNe are inherently of low surface brightness and so become essentially undetectable at larger distances in the Galactic plane where interstellar extinction becomes large. Hence, to be still visible they are likely to be relatively local (<2 kpc). It is important to find evolved PNe and their CSPN to sample CSPN evolution in the critical transition from PN to white dwarf (e.g. Napiwotzki 1995). Evolved PNe also provide sensitive probes of the PN–ISM interface on a range of spatial scales (Tweedy & Kwitter 1994), meriting detailed study (e.g. Xilouris et al. 1996; Corradi et al. 1997). Ciardullo et al. (1999) give compelling reasons why it is important to identify old remnant PNe, especially in relation to the 'distance scale' problem. Reconciling extinction, spectroscopic and trigonometric distances with model atmosphere distances remains a major problem in the field of PN research.

MASH has now greatly increased this number and found even more extreme examples (up to 0.5° across). We are currently obtaining additional narrow-band imaging of these nebulae, deeper optical spectroscopy, and broad-band (*UBVRI*) photometry of their central stars to establish a solid framework for new distance estimates to these local PNe (e.g. Frew & Parker 2005; Frew 2006). Such distances are vital to permit proper derivation of nebular and CSPN properties, as well as better estimates of the true space density and scaleheight of this evolved population. These data will also enable a much improved definition of the faint end of the PNLF which can be directly compared to those in other populations such as the Large Magellanic Cloud (e.g. Reid & Parker 2006a,b). Such a volume-limited sample will also allow the disc fraction of Type I PNe to be better determined (e.g. Frew, Parker & Russeil 2006).

8.2 Galactic bulge PNe

Assuming a common distance to PNe in the Galactic bulge permits estimates of mass, luminosity, age and temperature, vital parameters to study the underlying stellar population and PN evolutionary state. MASH has more than doubled the known Galactic bulge PN population with ∼400 more compact and extended bulge PNe than in the Strasbourg/ESO Catalogue (e.g. Peyaud et al. 2003, 2004; Peyaud 2005). The new sample relates to both extremes of the bulge PN population and will enable a more robust determination of the bulge PNLF for comparison with models and external galaxies (Parker, Acker et al. in preparation). MASH bulge PNe greatly augment the dynamical tracers for our Galaxy which will enable us to directly test theoretical kinematic features of bulge and bar. Peyaud (PhD, 2005) analysed the whole sample of galactic bulge PNe (405 MASH and 396 already known) to extract physical properties and precise kinematical parameters of the bulge leading to an exploration of bulge dynamics with *N*-body models (e.g. see Peyaud et al. 2006).

8.3 Study of WR central stars of Galactic PNe

Wolf–Rayet, [WR], CSPNe are rare; 56 were catalogued by Jeffery et al. (1996) whilst Acker & Neiner (2003) catalogued 121 emission-line CSPN which included both weak emission-line stars (WELS) and [WR] types. Górny et al. (2004) have recently discovered an additional 14 new [WR] and 15 WELS. MASH spectroscopic follow-up of CSPN has led to 20 such objects being discovered so far (e.g. Morgan, Parker & Russeil 2001; Parker & Morgan 2003), including PM5, the sole Galactic PN discovered with a WN central star (Morgan, Parker & Cohen 2003). All other [WR] CSPNe are WC/WO-types or WELS (Tylenda, Acker & Stenholm 1993).

9 CONCLUSIONS

The MASH catalogue of 905 true, likely and possible PNe represents the single most significant addition to the Galactic PN population ever compiled. We provide accurate positions, angular size estimates in Hα (+[N II]) light, morphological classifications and complete follow-up spectroscopy for all entries in the catalogue. A key strength is that the new PNe have all been discovered from the same uniform, observational data to yield the most homogeneous sample of PNe yet created. Furthermore, MASH discoveries probe PNe across a broader evolutionary range than available previously. MASH PNe are typically more evolved, obscured, of larger angular extent, and of lower surface brightness than those in most other surveys. Despite this our fraction of bipolar PNe (∼12.5 per cent) agrees well with that reported by Corradi & Schwarz (1995) who found 14 per cent of 400 PNe to be bipolar.

The catalogue promises to impact many aspects of PN research not only via sheer statistical weight but crucially by sampling new parameter space, particularly at the highly evolved end. For the first time serious deficiencies in the PNLF can be addressed at the faint extremes, probing underrepresented evolutionary stages of PNe and their central stars. MASH offers an unrivalled platform for research in: late stellar evolution; CSPN mass-loss history; PN evolution; ISM interaction; ISM chemical enrichment; Galactic abundance gradients and Galactic bulge dynamics.

An ongoing programme of spectral measurements will provide additional scientific utility in the form of velocities, line ratios, flux estimates and, where possible, density and temperature determinations. A parallel programme of deep imaging to identify and measure

the PN central stars is also underway. These new data will be incorporated into future updates to the catalogue and the results will be summarized in further papers in the series. We invite the astronomical community to exploit this major new PN catalogue and would be grateful if this paper is referenced when using the MASH catalogue.

ACKNOWLEDGMENTS

The authors gratefully acknowledge the support of the AAO board, the Wide-Field Astronomy Unit at Edinburgh University, and the past AAO directors Russell Cannon and Brian Boyle for making the SHS, on which all these discoveries were based, possible. We thank Ian Bond for making his PSF matching difference imaging software available to the SHS. QAP thanks the South African Astronomical Observatory, Australian National University, European Southern Observatory and the UK and Australian telescope time allocation committees, PATT and ATAC, for consistently supporting the extensive programme of follow-up spectroscopy over several years. QAP and DJF also thank the Australian Science and Nuclear Technology Organization (ANSTO) via their Access to Major Research Facilities Programme and Macquarie University for providing observing support. MC thanks NASA for supporting his participation in MASH through LTSA grant NAG5-7936 and ADP grant NNG04GD43G with UC Berkeley. DJF and AEJP thank Macquarie University for the provision of PhD scholarships while MJP thanks PPARC for provision of a PhD studentship. RAHM thanks PPARC for observing support during this project.

Grateful thanks are also given to QAP's AAO vacation scholar Amanda Norton who reduced the 2001 May SAAO spectroscopic data. QAP also thanks the following Nuffield and senior honours project students at Edinburgh University who have contributed to the visual search for PN in several fields: Elise Laird, Sybil Kadel, Cheryl Simms, Laura Morgan, Laura Douglas, Massumeh Guyanapeh, Caroline Thomson, Anne Rowntree, Matt Jones and Edward Thomson. We thank David Riddle for clarification on a cometary globule contaminant. We thank Ella Hopewell for the addition of a compact PN from an independent spectroscopic 6dF run and Retha Pretorius for two compact PN from the SHS. We thank Milorad Stupar (MS) for assisting QAP with the 2004 June 2.3-m and 2004 July SAAO 1.9-m observing runs, respectively. BM thanks the AAO and Macquarie University for vacation scholarships which enabled the development of 'PNDR' and the reduction of several observing runs. Finally, QAP thanks Strasbourg Observatory of the Université Louis Pasteur and director Jean-Marie Hameury for supporting a series of visits between 2001 and 2006 and Prof. Mark Birkinshaw of Bristol University for visitor support in 2002 which have greatly contributed to the success of the project.

This study used data from the Southern Hα Sky Survey Atlas (SHASSA), which was produced with support from the National Science Foundation. This research has made use of the SIMBAD data base, operated at CDS, Strasbourg, France, and makes use of data products from the 2MASS, which is a joint project of the University of Massachusetts and the Infrared Processing and Analysis Center/California Institute of Technology, funded by the NASA and the US National Science Foundation.

REFERENCES

Acker A., Neiner C., 2003, A&A, 403, 659
Acker A., Stenholm B., 1990, A&AS, 86, 219
Acker A., Ochsenbein F., Stenholm B., Tylenda R., Marcout J., Schohn C., 1992, Strasbourg-ESO Catalogue of Galactic Planetary Nebulae. ESO, Garching
Acker A., Marcout J., Ochsenbein F., 1996, First Supplement to the SECPGN. Observatoire de Strasbourg
Beard S. M., MacGillivray H. T., Thanisch P. F., 1990, MNRAS, 247, 311
Beaulieu S. F., Dopita M. A., Freeman K. C., 1999, ApJ, 515, 610
Beer S. H., Vaughan A. E., 1999, PASA, 16, 134
Belczyński K., Mikolajewska J., Munari U., Ivison R. J., Friedjung M., 2000, A&AS, 146, 407
Bond I. A. et al., 2001, MNRAS, 327, 868
Boumis P., Paleologou E. V., Mavromatakis F., Papamastorakis J., 2003, MNRAS, 339, 735
Boumis P., Akras S., Xilouris E. M., Mavromatakis F., Kapakos E., Papamastorakis J., Goudis C. D., 2006, MNRAS, 367, 1551
Cantó J., 1981, in Kahn F. D. ed., Astrophys. Space Sci. Library, Vol. 91, Investigating the Universe. Reidel, Dordrecht, p. 95
Chu Y.-H., Gruendl R. A., Williams R. M., Gull T. R., Werner K., 2004, AJ, 128, 2357
Ciardullo R., Bond H. E., Sipior M. S., Fulton L. K., Zhang C.-Y., Sxhawfwe K. G., 1999, AJ, 118, 488
Cohen M., Parker Q. A., 2003, in Dopita M., Kwok S., Sutherland R. eds, IAU Symp. 109, Planetary Nebulae: Their Evolution and Role in the Universe. Astron. Soc. Pac., San Francisco, p. 33
Cohen M., Parker Q. A., Green A., 2005, MNRAS, 360, 1439
Corradi R. L. M., 1995, MNRAS, 276, 521
Corradi R. L. M., Schwarz H. E., 1993, A&A, 268, 714
Corradi R. L. M., Schwarz H. E., 1995, A&A, 293, 871
Corradi R. L. M., Villaver E., Mampaso A., Perinotto M., 1997, A&A, 324, 276
Corradi R. L. M., Brandi E., Ferrer O. E., Schwarz H. E., 1999, A&A, 343, 841
Corradi R. L. M. et al., 2005, in Szczerba R., Stasińska S., Górny S. K., eds, AIP Conf. Proc. 804, Planetary Nebulae as Astronomical Tools. Am. Inst. Phys., New York, p. 7
Drew J. et al., 2005, MNRAS, 362, 753
Fesen R. A., Blair W. P., Kirshner R. P., 1985, ApJ, 292, 29
Frew D. J., 2006, PhD thesis, Macquarie Univ.
Frew D. J., Parker Q. A., 2005, in Szczerba R., Stasińska G., Górny S., eds, AIP Conf. Proc. 804, Planetary Nebulae as Astronomical Tools, Am. Inst. Phys., New York, p. 11
Frew D. J., Parker Q. A., Russeil D., 2006, MNRAS, 372, 1081
Gaustad J. E., McCullough P. R., Rosing W., Van Buren D., 2001, PASP, 113, 1326
Górny S. K., Stasińska G., Escudero A. V., Costa R. D. D., 2004, A&A, 427, 231
Gutiérrez-Moreno A., Moreno H., Cortés G., 1995, PASP, 107, 462
Hambly N. C. et al., 2001a, MNRAS, 326, 1279
Hambly N. C., Irwin M. J., MacGillivray H. T., 2001b, MNRAS, 326, 1295
Henize K. G., 1967, ApJS, 14, 125
Hewett P. C., Irwin M. J., Skillman E. D., Foltz C. B., Willis J. P., Warren S. J., Walton N. A., 2003, ApJ, 599, 37
Iben I. J., 1995, Phys. Rep., 250, 2
Jacoby G. H., van de Steene G., 2004, A&A, 419, 563
Jeffery C. S., Heber U., Hill P. W., Dreizler S., Drilling J. S., 1996, in Jeffery C. S., Huber U., eds, ASP Conf. Ser. Vol. 96, Hydrogen-Deficient Stars. Astron. Soc. Pac., San Francisco, p. 471
Kaler J. B., 1981, ApJ, 250, 31
Kennicutt R. C., Bresolin F., French H., Martin P., 2000, ApJ, 537, 589
Kerber F., Lercher G., Weinberger R., 1996, A&AS, 119, 423
Kerber F., Roth M., Manchado A., Gröbner H., 1998, A&AS, 130, 501
Kerber F., Mignani R., Guglielmetti F., Wicenec A., 2003, A&A, 408, 1029
Kimeswenger S., 2001, Rev. Mex. Astron. Astrofis., 37, 115
Kohoutek L., 1983, in Flower D. R., ed., Proc. IAU Symp. 103, Planetary Nebulae. Reidel, Dordrecht, p. 17
Kohoutek L., 2001, Catalogue of Galactic Planetary Nebulae (Updated Version 2000). Abhandlungen Hamburger Sternwarte, XII

Kohoutek L., 2002, AN, 323, 57
Kohoutek L., Kühl D., 2002, AN, 323, 484
Köppen J., Acker A., Stenholm B., 1991, A&A, 248, 197
Kraan-Korteweg R. C., Fairall A. P., Woudt P. A., van den Steene G. C., 1996, A&A, 315, 549.
Larios G. R., Phillips J. P., 2005, MNRAS, 357, 732
Luo S. G., Condon J. J., Yin Q. F., 2005, ApJS, 159, 282
Maciel W. J., Costa R. D. D., 2003, in Dopita M., Kwok S., Sutherland R., eds, IAU Symp. 109, Planetary Nebulae: Their Evolution and Role in the Universe. Astron. Soc. Pac., San Francisco, p. 551
Mader S. L., Zealey W. J., Parker Q. A., Masheder M. R. W., 1999, MNRAS, 310, 331
Manchado A., 2004, in Meixner M., Kastner J. H., Balick B., Soker N., eds, ASP Conf. Proc. Vol., 313, Asymmetrical Planetary Nebulae III: Winds, Structure and the Thunderbird. Astron. Soc. Pac., San Francisco, p. 3
Melmer D., Weinberger R., 1990, MNRAS, 243, 236
Mikolajewska J., Acker A., Stenholm B., 1997, A&A, 327, 191
Morgan D. H., Parker Q. A., 1998, MNRAS, 296, 921
Morgan D. H., Parker Q. A., Russeil D., 2001, MNRAS, 322, 877
Morgan D. H., Parker Q. A., Cohen M., 2003, MNRAS, 346, 729
Napiwotzki R., 1995, Lecture Notes in Physics, 443, 176
Ochsenbein F., Bauer P., Marcout J., 2000, A&AS, 143, 23
Parker Q. A., 2000, AAO Newslett., 94, 9
Parker Q. A., Bland-Hawthorn J., 1998, PASA, 15, 33
Parker Q. A., Malin D. F., 1999, PASA, 16, 288
Parker Q. A., Morgan D. H., 2003, MNRAS, 341, 961
Parker Q. A., Phillipps S., 1998, A&G, 39, 4
Parker Q. A. et al., 2001, Edinburgh/AAO/Strasbourg H-alpha Planetary Nebula Catalogue, Version 1.0. CDS, Strasbourg, France
Parker Q. A. et al., 2003, in Dopita M., Kwok S., Sutherland R., eds, IAU Symp. 209, Planetary Nebulae: Their Evolution and Role in the Universe. Astron. Soc. Pac., San Francisco, p. 41
Parker Q. A., Frew D. J., Stupar M., 2004, AAO Newslett., 104, 9
Parker Q. A. et al., 2005, MNRAS, 362, 689
Perek L., Kohoutek L., 1967, Catalogue of Galactic Planetary Nebulae, parts 1–3. Acad. Publ. House Czech. Acad. Sci., 1
Peyaud A. E. J., 2005, PhD thesis, Macquarie Univ., Univ. Louis Pasteur de Strasbourg
Peyaud A. E. J., Acker A., Parker Q. A., 2003, in Combes F., Barret D., Contini T., Pagani L., eds, SF2A-2003: Semaine de l'Astrophysique Francaise. EdP-Sciences, Gif-sur-Yvette, p. 311
Peyaud A. E. J., Acker A., Parker Q. A., 2004, in Combes F., Barret D., Contini T., Meybadier F., Pagani L., eds, SF2A-2004: Semaine de l'Astrophysique Francaise. EdP-Sciences, Gif-sur-Yvette, p. 625
Peyaud A. E. J., Acker A., Parker Q. A., 2006, in Barlow M. J., Mendez R. H., eds, Proc. IAU Symp. 234, Planetary Nebulae in Our Galaxy and Beyond. Cambridge Univ. Press, Cambridge, in press
Pierce M. J., 2005, PhD thesis, Univ. Bristol
Pierce M. J., Frew D. J., Parker Q. A., Köppen J., 2004, PASA, 21, 334
Price S. D., Egan M. P., Carey S. J., Mizuno D., Kuchar T., 2001, AJ, 121, 2819
Ratag M. A., Pottash S. R., 1991, A&AS, 91, 481
Rauch T., Furlan E., Kerber F., Roth M., 2000, in Kastner J. H., Soker N., Rappaport S., eds, ASP Conf. Ser. Vol. 199, Asymmetrical Planetary Nebulae II: From Origins to Microstructures, Astron. Soc. Pac., San Francisco, p. 341
Reid W. A., Parker Q. A., 2006a, MNRAS, 365, 401
Reid W. A., Parker Q. A. 2006b, MNRAS, in press (doi:10.1111/j.1365-2966.2006.11087.x)
Riesgo-Tirado H., López J. A., 2002, Rev. Mex. Astron. Astrofis. Ser. Conf., 12, 174
Sabbadin F., D'Odorico S., 1976, A&A, 49, 119
Sabbadin F., Minello S., Bianchini A., 1977, A&A, 60, 147
Schmeja S., Kimeswenger S., 2001, A&A, 377, L18
Schwarz H. E., Corradi R. L. M., Stanghellini L., 1993, in Weinberger R., Acker A., eds, Proc. IAU Symp. 155, Planetary Nebulae. Kluwer, Dordrecht, p. 214
Sellwood J. A., 1993, in Hold S. S., Verter F., eds, AIP Conf. Proc. Vol. 278, Back to the Galaxy. Am. Inst. Phys., New York, p. 133
Soker N., 1997, ApJS, 112, 487
Soker N., 2002, A&A, 386, 885
Stenholm B., Acker A., 1987, A&AS, 68, 51
Stupar M., Parker Q. A., Filipovic M. D., Frew D. J., Bojičić I., Aschenbach B. 2006, MNRAS, submitted
Taylor K., Bailey J., Wilkins T., Shortridge K., Glazebrook K., 1996, in Jacoby G., Barnes J., eds, ASP. Conf. Ser. Vol. 101, Astronomical Data Analysis Software and Systems V. Astron. Soc. Pac., San Francisco, p. 195
Tweedy R. W., Kwitter K. B., 1994, AJ, 108, 188
Tweedy R. W., Kwitter K. B., 1996, ApJ, 107, 255
Tweedy R. W., Napiwotzki R., 1994, AJ, 108, 978
Tweedy R. W., Martos M. A., Noriega-Crespo A., 1995, ApJ, 447, 257
Tylenda R., Acker A., Stenholm B., 1993, A&AS, 102, 595
Van de Steene G. C., Pottash S. R., 1995, A&A, 299, 238
Watson F. G., Parker Q. A., Miziarski S., 1998, SPIE, 3355, 834
Weinberger R., Kerber K., Groebner H., 1997, A&A, 323, 963
Xilouris K. M., Papamastorakis J., Paleologou E., Terzian Y., 1996, A&A, 310, 603
Zijlstra A. A., Pottasch S. R., 1991, A&A, 243, 478

This paper has been typeset from a TEX/LATEX file prepared by the author.